European Journal of Pharmaceutical Sciences 161 (2021) 105817

Contents lists available at ScienceDirect

European Journal of Pharmaceutical Sciences

journal homepage: www.elsevier.com/locate/ejps

Enhanced solubility and biopharmaceutical performance of atorvastatin and metformin *via* electrospun polyvinylpyrrolidone-hyaluronic acid composite nanoparticles

Rabia Iqbal [1], Omer Salman Qureshi [2], Abid Mehmood Yousaf [3,*], Syed Atif Raza [4], Hafiz Shoaib Sarwar [1], Gul Shahnaz [5], Uzma Saleem [6], Muhammad Farhan Sohail [1,7,**]

[1] *Riphah Institute of Pharmaceutical Sciences (RIPS), Riphah International University, Lahore Campus, Lahore, 54000, Pakistan*
[2] *Department of Pharmacy, Faculty of Natural Sciences, Forman Christian College University, Lahore, 54000, Pakistan*
[3] *Department of Pharmacy, COMSAT University Islamabad, Lahore Campus, Lahore, 54000, Pakistan*
[4] *Punjab University College of Pharmacy, University of the Punjab, Lahore, 54000, Pakistan*
[5] *Department of Pharmacy, Faculty of Biological Sciences, Quaid-i-Azam University, Islamabad, Pakistan*
[6] *Department of Pharmacology, Faculty of Pharmacy, GC University, Faisalabad, Pakistan*
[7] *Department of Pharmacy, Faculty of Health and Medical Sciences, University of Copenhagen, Denmark*

ARTICLE INFO

Keywords:
Atorvastatin
Electrospraying
Metformin
Nanoparticles
Permeability
Solubility

ABSTRACT

The study was aimed to improve the aqueous solubility of atorvastatin (AT) and ameliorate permeability of metformin (MT) in a combination formulation, improving their oral bioavailability. Several AT-MT loaded polyvinylpyrrolidone (PVP) and hyaluronic acid (HA) based nanoparticles were prepared through electrospraying method (ES-NPs), and tested for physicochemical, *in vitro,* and *in vivo* parameters. Among the trialed formulations, a sample consisting of AT, MT, PVP, and HA at the weight ratio of 1/6.25/3.75/15 furnished the most satisfying solubility and release rate results. It enhanced approximately 10.3-fold and 3.6-fold solubility of AT as compared with AT powder and marketed product (Lipilow) in phosphate buffer pH = 6.8, respectively. Whereas, permeation of MT was 1.60-fold and 1.47-fold improved as compared with MT powder and marketed product (Glucophage), respectively. As compared with Lipilow, AUC $_{(0-\infty)}$ and C_{max} of AT with ES-NPs in rats were improved to 3.6-fold and 3.2-fold, respectively. Similarly, as compared with Glucophage, AUC $_{(0-\infty)}$ and C_{max} of MT were improved to 2.3-fold and 1.8-fold, respectively. Thus, ES-NPs significantly enhanced the solubility of AT (a BCS class II drug) and permeability of MT (a BCS class III drug) and might be a promising drug delivery system for co-delivery of these drugs.

1. Introduction

Biopharmaceutics classification system (BCS) class II, class III and class IV drugs have always been a strong candidate for research in pharmaceutical sciences aimed to improve their solubility and/or permeation following oral administration. Both the aqueous solubility and permeability are imperative factors for adequate absorption and bioavailability of a drug administered via the oral route, and play a vital role in the formulation development process (Hu et al., 2004). Poor aqueous solubility is one of the major challenges for many pharmaceutical companies. About 60-70%, 5-10%, and 10-20% of the drug molecules under development belong to BCS class II, class III, and class IV, respectively. Thus, 70-90% of new chemical entities (NCEs) are facing poor aqueous solubility problems while 15-30% of them have permeation hindrance (Nikolakakis and Partheniadis, 2017).

Several approaches have successfully been employed for the enhancement of solubility and permeation which include micronization (Zu et al., 2014), ordered mixture (Nyström and Westerberg, 1986), roll mixing (Nozawa et al., 1984), complexation (JS et al., 2010), microemulsions (Solanki et al., 2012), self-emulsifying drug delivery systems

* Correspondence: Abid Mehmood Yousaf, PhD, Assistant Professor, Department of Pharmacy, COMSAT University Islamabad, Lahore Campus, Lahore, 54000, Pakistan. Tel: +92-300-4774147.
** Correspondence: Muhammad Farhan Sohail, PhD, Associate Professor, Riphah Institute of Pharmaceutical Sciences (RIPS), Riphah International University, Lahore Campus, Lahore, 54000, Pakistan. Tel: +92-344-4120001.
E-mail addresses: abid.ucp@hotmail.com (A.M. Yousaf), farmacist.pk@gmail.com (M.F. Sohail).

https://doi.org/10.1016/j.ejps.2021.105817
Received 13 November 2020; Received in revised form 16 March 2021; Accepted 18 March 2021
Available online 20 March 2021

(SEDDS) (Reddy et al., 2014) and solid dispersions (Sareen et al., 2012). The advancement in nanotechnology has introduced new avenues in drug delivery science through multifaceted applications of nanoparticles, nanosuspensions, nanofibers, nanospherules, niosomes, and so on. The electrospraying method or electrohydrodynamic technique (EHD) has emerged as a promising method for the production of nanoparticles where all the formulation components are simply dissolved in the solvent and the final clear solution is then sprayed to produce ES-NPs. The resultant ES-NPs are usually spherical containing evenly distributed drug molecules in the polymeric matrix. Natural polymers impart excellent properties of biodegradation and biocompatibility (Sapkal et al., 2013). As compared to other conventional methods of nanoparticle fabrication, electrospraying provides several advantages such as higher drug loading efficiency, simplicity, single-step facile process, increased surface area (Jahangiri and Adibkia, 2016), and narrow particle-size distribution or (Din et al., 2017) tendency towards monodispersity (Jaworek and Sobczyk, 2008). EHD possesses a fairly broad scope in several biomedical disciplines and drug delivery encompassing inhalation therapy (Tang and Gomez, 1994), tissue engineering (Dersch et al., 2007), wound dressing applications (Hameed et al., 2020), chemotherapy (Din et al., 2017), antihyperlipidemic therapy (Yousaf et al., 2016) and (Sun et al., 2020b), analgesia (Mustapha et al., 2016) and protein delivery (Sridhar and Ramakrishna, 2013).

Cardiovascular conditions and type-II diabetes mellitus (T2DM) are usually found comorbid. In the patients suffering from diabetes and dyslipidemia simultaneously, increased concentrations of triglyceride (TG), the elevated prevalence of low-density lipoprotein cholesterol (LDL-C), and downregulation of high-density lipoprotein cholesterol (HDL-C) (Wu and Parhofer, 2014) have been detected. These factors ultimately lead to atherosclerosis and associated complications such as thrombosis, infarction, angina, heart attack, and stroke (Grundy et al., 2004).

Metformin (MT) is the drug of choice in treating T2DM and statins are the first choice of treatment in diabetic dyslipidemia patients (Mortensen et al., 2016). A clinical study comprised of 12 weeks of administration of metformin in T2DM patients revealed beneficial effects on the cardiovascular condition. Moreover, insulin resistance in T2DM patients is often found in association with dyslipidemia which certainly augments the risk factors for myocardial infarction. Furthermore, single therapy with statins in patients with dyslipidemia leads to an increased incidence of T2DM (Sattar et al., 2010). Thus, statin therapy in T2DM patients is important even without cardiovascular conditions because both the drugs, metformin and statins, influence glucose and lipids metabolism; accordingly, they are mostly prescribed in T2DM patients.

Atorvastatin (AT) is commonly prescribed as a calcium salt to treat antihyperlipidemic. It is a BCS class II entity and exhibits a very poor aqueous solubility (< 0.1 mg/mL) (Shayanfar et al., 2013). It is a highly lipophilic molecule with a *log P* = 6.36 and a molecular weight of about 1209.42 *Da* (Malinowski, 1998). Owing to low solubility in the aqueous media, high first-pass metabolic effect, and possessing crystalline physiognomies, atorvastatin calcium furnishes low bioavailability (~ 12%) following oral administration.

Metformin (MT) is clinically used as an antihyperglycemic agent in the management of T2DM. It is a BCS class III substance and shows inadequate permeation following oral administration. At physiologic pH, it becomes protonated and has a high affinity for the intestinal wall (negatively charged); thus, leading to its decreased permeation across membranes (Stepensky et al., 2001).

Hyaluronic acid (HA) and polyvinylpyrrolidone (PVP), being biocompatible and biodegradable polymeric matrices, are well renowned for drug delivery excipients. HA is a complex molecule of disaccharide components, *D*-glucuronic acid, and *N*-acetylglucosamine, linked by interchanging β-1,4 and β-1,3 glycosidic linkages (Cyphert et al., 2015). HA is water soluble with high viscoelasticity and can combine with receptors on the surface of the cell. It can significantly boost the bioavailability of poorly soluble drugs by efficient drug wetting. PVP is a hydrophilic polymer with high solubility in a wide range of organic solvents as well. PVP has been shown to improve the wettability of several hydrophobic compounds depending on their molecular weight (Yousaf et al., 2016). It has been noticed that larger molecular weight PVP demonstrates a slower dissolution rate owing to the higher viscosity (Leuner and Dressman, 2000).

In the present study, AT-MT loaded HA-PVP polymeric ES-NPs were prepared for concomitant oral administration of the drugs with enhanced solubility and permeability through the oral route to achieve an ameliorated bioavailability. Saturation solubilities and release rates of the drugs were assessed in the aqueous media at various pH. *Ex vivo* permeation studies were performed using the goat intestine. Other *in vitro* characterizations involved particle-size determination, FTIR, DSC, and SEM. For *in vivo* oral bioavailability and biopharmaceutical performance testing, white albino laboratory rats (Sprague-Dawley rats) were exploited. Pharmacokinetic parameters such as AUC, $C_{max,}$ and T_{max} were considered for comparisons of bioavailabilities.

2. Materials and Methods

2.1. Materials

Atorvastatin calcium (Biocon Ltd., Bangalore, KA, India); metformin HCl (Aarti Drugs Ltd., Tarapur, MH, India); polyvinylpyrrolidone (PVP-K30), hyaluronic acid (MW 8000-15000), sodium hydroxide, hydrochloric acid, potassium chloride, and potassium dihydrogen phosphate (Sigma-Aldrich, St. Louis, MO, USA); magnesium sulfate, sodium sulfate heptahydrate, sodium hydrogen carbonate, glucose, calcium chloride, polysorbate 20, chloride, and methanol HPLC grade (Merck Co., Billerica, Middlesex-County, MO, USA); ethanol HPLC grade (BDH® chemicals, USA).

2.2. Process optimization and microscopic evaluation

Optimization of the process was done by electrospraying the prepared clear solutions at different process parameters such as flow rate, needle-collector distance, applied voltage, and viscosity of the solution. A prepared solution was run for about 3-5 min at each set of parameters, and the product obtained was visually observed using an optical microscope (Optika-micros IM3, *via* Riga, Ponteranica, Italy). The rheological studies were employed, for viscosity analysis, using cone and plate type rheometer (TA Instruments Ltd. AR 1500). The studies were performed at 25C, with the shear rate increased from 0-1000 S^{-1} over 1 min and decreased to 0 S^{-1} in 1 min.

2.3. Preparation of ES-NPs

Compositions of formulations are shown in **Table 1**. For a formulation, accurately weighed quantities of AT, MT, PVP, and HA was thoroughly dissolved in an alcoholic mixture consisting of ethanol/methanol (1/1, v/v). For obtaining a transparent compound solution of components, stirring was performed for 1 h prior to subjecting the solution to the electrospraying process (Sun et al., 2020a). Electrospraying equipment (ESR-100-Nano-NC; Seoul, Gyeonggi-do, South Korea) was consisting of a 50 mL capacity syringe (Hamilton Co.; Reno, NV, USA) fitted with a 21-*G* stainless steel spraying nozzle, syringe pump, high voltage source with the regulator, and a metallic product-collector. Electrospraying was conducted following the pre-optimized parameters of voltage (22 kV), flow rate (0.5 mL/h), and distance between the nozzle tip and the product-collector (15 cm). The piling of ES-NPs on the aluminum foil was done by sweeping with the help of a soft brush. The percentage yield was calculated from the collected NPs. Each ES-NPs formulation was transferred into an air-tight and well-dried microtube with the help of same brush and preserved until further

Table 1
Compositions of AT and MT loaded PVP-HA composite ES-NPs.

Components (mg)	F1	F2	F3	F4	F5	F6	F3 (1%)	F5 (1%)
Atorvastatin Calcium	80	80	80	80	80	80	80	80
Metformin HCl	500	500	500	500	500	500	500	500
Polyvinylpyrrolidone	1500	1200	900	600	300	0	900	300
Hyaluronic Acid	0	300	600	900	1200	1500	600	1200
Polysorbate 20	-	-	-	-	-	-	21	21
% Yield of ES-NPs	78.5	88.5	92.4	84.6	94.5	85.2	93.2	94.0

experimentations.

2.4. Saturation solubility studies

Saturation solubility tests were performed using distilled water and buffer solutions (pH = 1.2 and pH = 6.8) as an aqueous media. For a mixture of plain drug powders or an ES-NPs formulation, an ample quantity was added to 1 mL of an aqueous medium in a 2 mL capacity Eppendorf microtube. Then, the microtube was tightly closed, vortexed for 2 min using a vortex-mixer (MyLab™ SLV-6, SeouLin Bioscience, Seongnam-si, Gyeonggi-do, South Korea), and sonicated for 20 min subsequently. The tubes were centrifuged (Sigma 2-16KC, Sigma Laborzentrifugen, An der Uteren Söse, Osterode am Harz, Germany) at 8000 rpm for 10 min. The supernatant was filtered by 0.45 μm syringe-filter and analyzed through HPLC following the method described below. (Yousaf et al., 2019).

2.5. HPLC method

An in-house simultaneous detection method, developed and validated by CCL Pharmaceuticals (Lahore, Pakistan), was adopted for the quantification of AT and MT. A reverse-phase HPLC (RP-HPLC) method was applied using an HPLC system equipped with a PDA detector (Agilent Technologies, USA) These drugs were separated by using a C-8 column (250 × 4.6 mm, 5-μm). The mobile phase was consisting of acetonitrile and phosphate buffer (pH = 3.0) at a volume ratio of 60/40. The mobile phase flow rate was set at 1 mL/min and column oven temperature was maintained at 25 ± 0.5°C. A 25 μL aliquot was injected and eluent assayed by the system at 235 nm wavelength. The retention time was observed as 2.96 and 5.21 min for MT and AT, respectively. The limit of detection (LOD) and limit of quantification (LOQ) for MT and AT were found to be 15.4 and 18.2 μg/mL and 14.6 and 16.3 μg/mL respectively. The linear equation for MT was y = 7827.7x + 6861.2 and for AT was y = 13771.9x + 19727.4.

2.6. Particle-size distribution, zeta potential, and polydispersity index analysis

The particle-size distribution, zeta potential, and polydispersity index (PDI) were determined using a Zetananosizer (Malvern Instruments, Malvern, Worcestershire, UK). The dried ES-NPs were suspended in water and the sample was diluted 10-folds before analysis (Afzal et al., 2019).

2.7. FTIR analysis

The FTIR spectrophotometer (Nicolet-6700; Pittsburgh, PA, USA), equipped with a diamond Smart Orbit ATR sampling accessory, was used to evaluate any likely incompatibility or possible interaction that might have to occur during the preparation process of ES-NPs. A small quantity of AT, MT, PVP, HA, physical mixture, or ES-NPs formulation was directly placed on the sample disk below the scanning probe. The spectra were recorded in the wavelength range of 4000-400 cm^{-1} with a resolution increment of 2 cm^{-1} (Sarwar et al., 2020). The physical mixture was prepared by simply triturating AT, MT, PVP, and HA (1/6.25/3.75/15, w/w/w/w) using a pestle and mortar.

2.8. Differential scanning calorimetry

Differential scanning calorimetry (DSC-Q20; TA Instruments, DE, USA) was employed for determining the crystalline intensity and thermal behavior of the samples. Each sample weighing about 10 mg was taken in an aluminum crucible (*Tzero*; TA Instruments, DE, USA) and snugly sealed with the lid. Then, this enclosed specimen was put inside the calorimeter with a vacant/hollow pan of the same substance as a reference. The enclosed calorimeter was gradually heated from 30°C to 300°C at a heating rate of 10°C/min and thermograms were recorded by the system. A constant supply of nitrogen gas (30 mL/min) in the calorimeter was ensured throughout the scanning process (Sohail et al., 2016).

2.9. Scanning electron microscopy

The contours and surface-texture quality of the particles were explored using a scanning electron microscope (*S*-4800; Hitachi, Japan). The samples were attached to the metallic sample disc using double-sided adhesive tape and coated with platinum by a turbo Ion-sputter coater (EMItech-*K*575*X*; Emitech Ltd., Strovolos, Nicosia, Cyprus) under 8×10^{-3} mbar vacuum pressure, turbo speed of 90%, and 20 *mA* current (Islam et al., 2020).

2.10. In vitro drug release analysis

USP paddle apparatus II was used to accomplish drug release studies. The plain AT/MT mixture (1/6.25, w/w) or an ES-NPs formulation equivalent to 3.2 mg AT and 20 mg MT, the commercial product Lipilow tablets equivalent to 3.2 mg AT, or marketed product Glucophage tablets equivalent to 20 mg MT was placed in a semi-permeable dialysis membrane of *MWCO* 12000 *Da*. The ends of the membranes were tightly closed to prevent any leakage. Then, the sample-loaded dialysis pouch, enclosed in a sinker, was dipped in 900 mL of an aqueous release medium (distilled water, buffer solution pH = 1.2 or buffer solution pH = 6.8) which was pre-warmed and maintained at 37 ± 0.5°C. The paddle rotation was set at 50 rpm. At pre-defined intervals, 3 mL of the release medium was sampled and filtered through a 0.45 μm syringe-filter. The filtrate was analyzed through RP-HPLC using an HPLC system described in section 2.4 (Mustapha et al., 2016).

2.10.1. Model-Independent methods

Comparison of release profiles of the ES-NPs, commercial products, and pure drugs was done using the factor of difference (f_1) and factor of similarity (f_2). The factor of difference determines the (%) difference between test and reference curves at each time. For the two curves to be perceived as comparable, f_1 should be approximate to zero (0-15) and f_2 should be close to 100 (50-100) (Zhang et al., 2010).

2.10.2. Model-Dependent methods

Mathematical kinetic models were applied to release data using DDSolver, a free MS Excel Add-in, for exploring a potential mechanism for drug release from the relevant drug delivery system (Kumar et al.,

2015).

2.11. Ex vivo permeability studies

2.11.1. Preparation of ES-NPs formulations for permeability test

Based upon the results of solubility and drug release evaluations, the formulations exhibiting the maximum solubility and release were selected for *ex vivo* permeation tests. For each selected formulation, AT, MT, PVP, HA, and polysorbate 20 (0.5% or 1%) were thoroughly dissolved in an alcoholic mixture consisting of ethanol/methanol (1/1, v/v) to get a clear solution. Subsequently, the compound solution was subjected to electrospraying following the method as described above in section 2.4 (Dimitrijevic et al., 2000).

2.11.2. Isolation of goat intestine

Krebs-Ringer solution was set by adding accurately weighed NaCl (6.3 g), KCl (0.35 g), $CaCl_2$ (0.14 g), KH_2PO_4 (0.16 g), $MgSO_4.7H_2O$ (0.15 g), $NaHCO_3$ (2.1 g), and glucose (5 g) to 1 L of distilled water. The intestinal lumen of freshly excised goat intestine was carefully cleaned by rinsing with phosphate buffer pH 6.8. A 6 cm intestinal segment was removed and placed between the donor and recipient chambers of the Franz diffusion cell (Chaudhari et al., 2016).

2.11.3. Franz diffusion cell

Franz diffusion cell was used to accomplish the permeability test. 1 mL solution of plain AT/MT mixture (1/6.25, w/w) or an ES-NPs formulation equivalent to 3.2 mg AT and 20 mg MT, the commercial product Lipilow tablets equivalent to 3.2 mg AT, or marketed product Glucophage tablets equivalent to 20 mg MT was placed in the donor segment of the Franz diffusion cell fixed with an intestinal segment of approximately 6 cm with an effective diffusion area of 1.038 cm^2. For the commercial tablets, the tablets were crushed and assayed. The weight of crushed tablets, equivalent to having 3.2 mg AT and 20 mg MT, was taken in the donor compartment. The volume of phosphate buffer (pH 6.8) in the donor compartment was 2 mL. The receptor compartment was filled with 9 mL of phosphate buffer (pH 6.8) maintained at 37 ± 0.5°C and stirred at 50 rpm. A 500 µL sample was removed at each fixed time point (30, 60, 90, 120, 150, and 180 min) and was replaced with a fresh medium. The withdrawn sample was diluted and analyzed using the HPLC method as described above in section 2.4. The apparent permeability (P_{app}), flux, and enhancement ratio (ER) were calculated using the equations mentioned below (Ghafar et al., 2020).

$$Papp = \left(\frac{V_A}{Area} X\ Time\right) X \left(\frac{[drug]_{acceptor}}{[drug]_{donor}}\right)$$

Where, V_A= volume in the acceptor section, area= intestinal membrane surface area, and time= Total transport time.

$$Flux\ (J) = Papp\ X\ CD$$

Where, CD = Concentration of the donor solution

$$Enhancement\ Ratio(ER) = \frac{Papp\ of\ formulation}{Papp\ of\ control}$$

2.12. Pharmacokinetic studies

This study was done with 18 healthy albino rats (300-500 g) following the approved protocol of the Research Ethical Committee (REC) of Riphah International University (Protocol No. REC-2020-42) based on the U.K. Animals (Scientific Procedures) Act, 1986 and associated guidelines, EU Directive 2010/63/EU for animal experiments and National Institutes of Health guide for the care and use of laboratory animals (NIH Publications No. 8023, revised 1978). The rats were divided into 3 equal groups (n = 6) and were kept on a standard diet. The 1st group received ES-NPs formulation F5-1% equivalent to 10 mg AT and 62.5 mg MT, the 2nd group received a Lipilow tablet equivalent to 10 mg AT and the 3rd group received a Glucophage tablet equivalent to 62.5 mg MT. The tablets were crushed and assayed. The weight of crushed tablets, equivalent to having 10 mg AT and 62.5 mg MT, was suspended in the water. All the formulations were suspended in 2 mL water and orally administered using a gavage needle. Blood samples (0.3 mL) were collected from the right femoral artery of each cannulated rat at predetermined intervals using heparinized syringes and poured into heparinized Eppendorf microtubes. Each blood sample was centrifuged at 9000 rpm for 10 min and plasma was transferred to separate microtubes. The samples were then analyzed through the HPLC method as described in section 2.4. PKSolver, a free MS Excel add-in, was used to calculate various pharmacokinetic parameters (Baloch et al., 2019).

2.13. Statistical Analysis

The statistical analysis was done by using SPSS (version-23.0; IBM-corp). Statistical significance ($p < 0.05$) was determined among the optimized formulation, pure drugs, and commercial product by using ANOVA followed by Post Hoc Tukey multiple comparison analysis. The results are presented as mean ± S.D. of at least 3 experiments unless stated otherwise (Wang et al., 2016).

3. Results and Discussion

Solubility and permeability of BCS class II, class III, and class IV drugs can be ameliorated through several novel techniques that are well reported for many drugs. Electrospraying is a simple, robust, bottom-up, highly customizable method for the development of mono-disperse polymeric NPs with several advantages (Jaworek, 2007).

In this study, clear homogeneous solutions of AT and MT were successfully incorporated in the polymeric solution of PVP and HA. The resultant compound solution was electrosprayed employing the optimized conditions for the fabrication of AT-MT loaded PVP-HA polymeric composite nanoparticles. Various process optimization attempts have been shown in Figure 1. Polymeric substances (PVP and HA) were selected owing to their well-established solubilization properties (Yousaf et al., 2015). PVP is a biodegradable, biocompatible polymer with significant lyophilization and solubility enhancement properties (Ibrahim and Klingner, 2020). PVP is involved in the delayed crystallization of loaded drugs resulted in increased dissolution rates (Franco and De Marco, 2020). Hyaluronic acid employed as a polymer in various micro and nano-scale drug delivery systems has been reported extensively. Likewise, PVP hyaluronic acid exhibits non-toxicity, non-immunogenicity, biocompatibility along with biodegradability (Snetkov et al., 2019). The combination of PVP and HA is unique to induce the advantages of both polymers and flexibility in the polymeric network within nanoparticles to maintain their shape and structure.

Electrospraying or electrohydrodynamic jetting is an advanced, effective, relatively simple, and cross-functional technology for the fabrication of various types of particles and fibers. This technique is mainly famous for the preparation of nano- and microscale fibers. However, researchers have utilized this technology for the development of polymeric nanoparticles by exploring the optimization of various process and formulation parameters (Snetkov et al., 2019).

Six different spraying solutions were prepared for ES-NPs and their viscosity was determined *via* viscometer. The results for viscosity showed the maximum viscosity of 16.18 ± 0.741 Pa s for F6 formulation (1:1, drugs: polymers) 10 mL solution, and the lowest was found to be 2.47 ± 0.360 Pa s for F5 formulation. The other formulations showed viscosity of 9.33 ± 0.257 Pa s for 15 mL solution, 2.64 ± 0.366 Pa s for F1 formulation, 2.41 ± 0.063 Pa s for F2 formulation, 2.803 ± 0.293 Pa s for F3 formulation, 2.726 ± 0.069 Pa s for F4 formulation, and 2.646 ± 0.250 Pa s for F6 formulation.

Optimization of the process was done by running the prepared solution at different process parameters such as flow rate (0.9 and 0.5 mL/

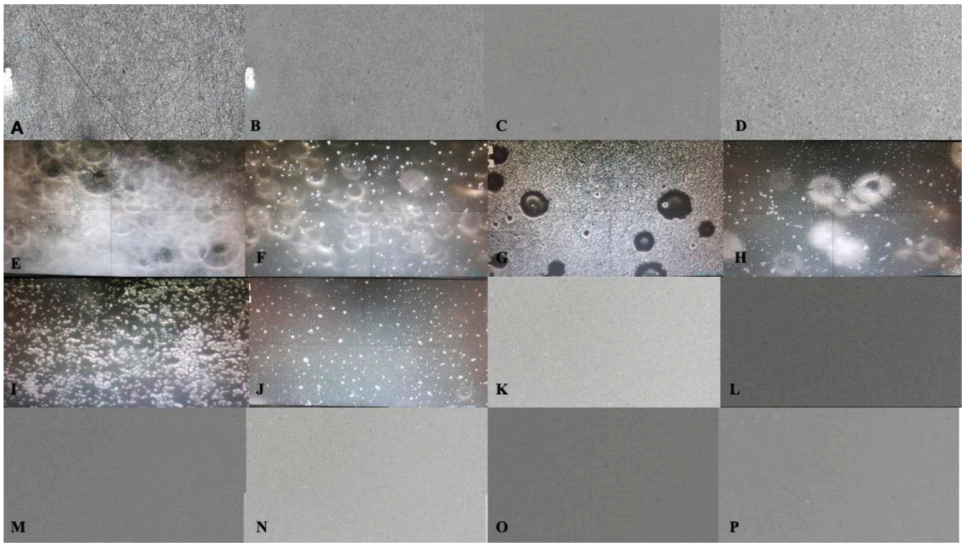

Figure 1. Representing microscopic images (40x) of 10 mL solution at different distance, flow rate and applied voltage: (**A**) 10 cm, 0.9 mL/hr, 15 kV; (**B**) 12 cm, 0.5 mL/hr, 19 kV; (**C**) 12 cm, 0.5 mL/hr, 17 kV). For 15 mL solution: (**D**) 12 cm, 1.5 mL/hr, 15 kV. For 20 mL solution: (**E**) 8 cm, 1.5 mL/hr, 15 kV; (**F**) 10 cm, 2 mL/hr, 17 kV; (**G**) 10 cm, 1 mL/hr, 10 kV; (**H**) 8 cm, 1 mL/hr, 15 kV; (**I**) 10 cm, 0.8 mL/hr, 25 kV; (**J**) 15 cm, 0.5 mL/hr, 20 kV and optimized parameters for all the nanoparticles formulations i.e., **K**(F1) to **P**(F6) were found to be 15 cm needle to collector distance, 0.5 mL/hr flow rate and 22 kV applied voltage respectively

h), needle and product-collector distance (10 and 12 cm), applied voltage (15, 17, 19, and 22 kV), and viscosity of the solution. For a 10 mL solution, three sets of conditions were applied, and the results are shown in Figure 1. With a 10 mL solution, fibers were seen in microscopic images due to the high viscosity of the solution indicating the process of electrospraying for the synthesis of fibers. Therefore, the prepared solution was diluted with 5 mL, and the process was run at three different parameters to get the optimized one for desirable particles. The resultant microscopic image of the sample at 12 cm distance, 0.5 mL/h flow rate, and 15 kV voltage are given in Figure 1 which showed that the product obtained was beaded fibers which indicated the need for further dilution of the solution and a transition from electrospinning to electrospraying process. Therefore, the solution was diluted further with 5 mL solvent to make it 20 mL (1:1 diluted). This diluted solution was again electrospraying at different parameters for optimization of the ES process. The results given in **Figure 1** showed the spherical structures indicating the preparation of ES-NPs.

The optimized parameters obtained were 15 cm needle-to-collector distance, 0.5 mL/h flow rate, and 22 kV voltage which produced ES-NPs. The percentage yield of the ES-NPs obtained from various formulation trials is given in **Table 1**. The yield varies between 78-94%, with the maximum value of 94.5% and minimum value of 78.5% shown by Formulation F5 and F1 respectively. The percentage yield remained almost the same for formulation F3 and F5 after incorporation of span-20.

PVP and HA polymers have been used to increase drug solubilities (Franco and De Marco, 2020). The influence of relative quantities of PVP and HA on the solubility (**Table 2**) and release behavior of the drugs in formulations was investigated. The results of ES-NPs for AT saturation solubility in three different solvents are shown in Figure 2**A.** Amongst all the ES-NPs formulations, F5 furnished the maximum solubility of AT in all the tested aqueous media. As compared to plain AT powder, enhancement in solubility of AT by F5 in distilled water, phosphate buffer (pH = 1.2), and phosphate buffer (pH = 6.8) was 9.6-fold, 5.38-fold, and 10.26-fold, respectively. The influence of ES-NPs formulations on the saturation solubility of MT is shown in Figure 2B. As compared to plain MT powder, enhancement in solubility of MT by F5 in the same 3 media was 1.12-fold, 1.22-fold, and 1.13-fold respectively. The presence of PVP alone in formulation F1 ameliorated ~6-fold solubility of AT as compared to plain AT powder. This suggested that PVP had a significant effect on the solubility of the drug. As the relative quantity of HA in a fixed quantity of PVP-HA mixture gradually increased in formulations F2-F5, the solubility of AT was gradually enhanced as well. This proved that HA also contributed to increasing the solubility of AT. As the quantity of PVP vanished in formulation F6, the solubility of AT suddenly decreased. This suggested that both PVP and HA exerted a synergistic effect on the solubility of AT in the PVP-HA polymeric composite. In particular, formulation F5, having PVP/HA (1/4, w/w), furnished the highest apparent solubility of AT amongst all the trialed formulations. As compared with the marketed product (Lipilow), AT solubility enhancement was about 3.5-fold with ES-NPs formulation F5. Moreover, a comparison of formulation F1 and F6 revealed that HA had a more persistent effect on amelioration of the solubility of AT than PVP. Also, the solubility of AT remained less in phosphate buffer (pH 1.2) than phosphate buffer (pH 6.8). This suggested that the solubility of AT was dependent on pH. The improvement in the solubility of AT (a poorly soluble drug, BCS class II) might be ascribed to the increased wettability of the drug by the hydrophilic

Table 2
Saturation solubility of atorvastatin and metformin in distilled water, phosphate buffer pH 1.2 and pH 6.8. The results are presented as the mean ± S.D. (n = 3).

	Atorvastatin (μg/mL)			Metformin (μg/mL)		
	Water	PB (pH 1.2)	PB (pH 6.8)	Water	PB (pH 1.2)	PB (pH 6.8)
Drug	24.44 ± 7.40	21.38 ± 4.48	28.05 ± 2.52	128.31 ± 6.56	111.25 ± 5.32	134.46 ± 3.71
Market Product	36.98 ± 5.98	34.98 ± 4.77	58.77 ± 4.99	131.66 ± 5.87	118.85 ± 5.40	137.98 ± 4.89
F1	120.18 ± 9.33	76.90 ± 5.85	156.18 ± 7.12	130.05 ± 5.13	120.83 ± 4.12	133.43 ± 3.79
F2	156.17 ± 9.89	83.16 ± 5.65	183.07 ± 8.68	142.01 ± 6.19	111.04 ± 6.92	135.84 ± 3.81
F3	184.19 ± 7.07	90.06 ± 2.73	205.25 ± 4.67	135.65 ± 4.45	124.79 ± 5.16	152.27 ± 5.57
F4	199.71 ± 4.57	103.01 ± 4.22	219.87 ± 6.53	132.45 ± 5.33	119.58 ± 7.22	138.62 ± 4.47
F5	234.33 ± 6.94	114.79 5.85	287.81 ± 7.57	143.91 ± 5.47	135.65 ± 8.10	148.73 ± 2.91
F6	96.41 ± 3.60	62.03 ± 3.15	137.59 ± 6.74	111.79 ± 3.88	111.04 ± 5.21	132.05 ± 4.87
F5-1%	242.78 ± 5.99	122.35 ± 4.98	293.67 ± 4.88	147.78 ±5.77	139.67 ± 5.48	156.67 ± 5.39
F3-1%	237.87 ± 4.89	117.48 ± 5.89	289.79 ± 5.23	138.68 ± 4.87	137.94 ± 4.90	152.89 ± 4.88

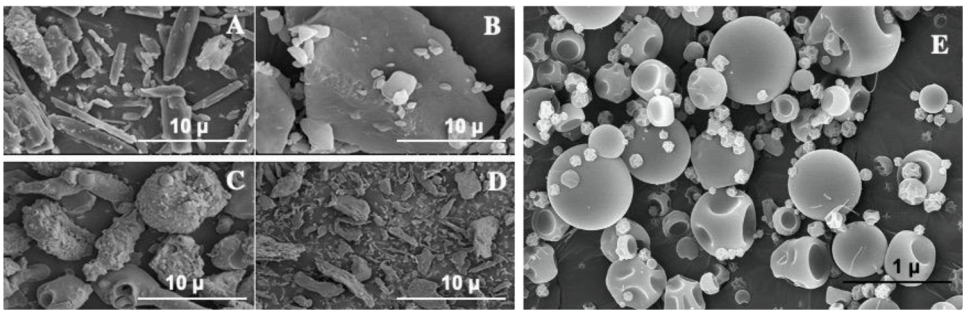

Figure 2. SEM images: (A) atorvastatin plain drug powder, (B) metformin plain drug powder, (C) PVP K-30, (D) hyaluronic acid, (E) ES-NPs formulation F5.

polymeric composite (Yousaf et al., 2016). MT is a BCS class III drug that has a permeability issue instead of a solubility problem; therefore, its solubility results were not significantly different from each other in all tested cases. Among all the formulations, F5 culminated in optimum solubility as compared with pure MT powder. The formulations F3 and F5 were reproduced with the additon of 1% span 20. The results of solubility of AT showed significant increase in the prsence of span 20 as compared to MT as shown in table 2 and table 3 respectively.

The electrospinning technique is famous for providing various nanoparticulated drug delivery systems with a narrow particle-size distribution. The hydrodynamic diameter of ES-NPs was found to be in the range of 380-420 nm and the PDI values ranging from 0.378 to 0.417. Out of 6 trials, formulation F5 showed the most desirable features as the particle-size was 410 nm with a slightly high PDI of 0.378, indicating polydispersity of synthesized ES-NPs. The surface charge on ES-NPs measured as zeta potential contributes to the physical stability of colloidal dispersions. Electrostatic repulsion induced by high surface charge prevents the formation of ES-NPs aggregates and ensures physical stability during storage. The ES-NPs of F5 showed a surface zeta potential of – 28 KeV. Also, there was no significant difference among the zeta potential values of blank ES-NPs and AT-MT loaded ES-NPs, suggesting that drug loading into the nanoparticles did not effectively alter the surface charge. The negative value of surface charge induces a significant electrostatic repulsion and prevents the formation of aggregates, thus, ensures physical stability during storage in colloidal state or during other evaluations both *in vitro* and *in vivo*. The absolute zeta potential value of about ± 30 mV is high enough to provide the storage stability of nanoparticles (Zeb et al., 2017).

In the scanning electron micrographs, AT (**Figure 2A**) and MT (**Figure 2B**) appeared as large crystals, whereas, the PVP (**Figure 2C**) and HA (**Figure 2D**) also showed irregular contours and rough surfaces of their respective particles. On the other hand, ES-NPs formulation F5 was consisting of smooth-surfaced particles with well-defined spherical contours and bearing 2-3 dimples on the surface (**Figure 2E**). This was owing to the final transparent solution which was subjected to electrospraying. An absolutely clear solution suggested that all the components were completely dissolved and molecularly intermingled. Besides, the presence of dimples on the surface of a particle might be owing to prompt drying. Thus, electrospraying technique improved the surface quality and contours of the particles and resulted in a reduction in particulate dimensions or more exposed surface area which in turn increased solubility, enhanced drug release, and improved biopharmaceutical performance of the laden drugs.

Table 3
Pharmacokinetic parameters of ES-NPs loaded with AT and MT in rats following oral administration. The results are presented as Mean ± S.D. (n = 6).

Parameter	Unit	Atorvastatin F5 (1%)	Lipilow	Metformin F5 (1%)	Glucophage
$t_{1/2}$	h	1.071 ± 1.47	0.709 ± 1.22	1.399 ± 1.31	0.969 ± 1.51
CL/F	(mg)/(µg/mL)/h	0.002 ± 0.66	0.008 ± 0.31	0.036 ± 0.27	0.084 ± 0.64
T_{max}	h	3.0 ± 1.25	2.0 ± 1.12	3.0 ± 1.02	2.0 ± 1.54
C_{max}	µg/mL	325.562 ± 24.66*	100.924 ± 21.63	192.727 ± 23.55	107.051 ± 10.47
AUC $_{(0\text{-}12)}$	(µg/mL).h	2923.433 ± 44.16*	849.912 ± 47.66	1745.801 ± 45.33	910.577 ± 45.76
AUC $_{(0\text{-}\infty)}$	(µg/mL).h	4442.855 ± 68.55*	1225.597 ± 87.44	2770.587 ±72.91*	1180.378 ± 78.17
MRT	h	18.161 ± 3.44*	10.254 ± 2.78	11.956 ± 3.15	8.535 ± 2.55

* ($p < 0.05$) significant difference.

The FTIR spectra (**Figure 3A**) showed no incompatibility among the various ingredients used for the ES-NPs synthesis. The peak in AT spectra appearing at 1316 cm^{-1} was an absorption peak of pyrrole (C-N stretch), that arising at 1377 cm^{-1} was related to fluoride (C-F stretch), and an absorption band of amide (N-H bend) appeared at 1580 cm^{-1}. A keto-amide (C=O stretch) notch arose at 1650 cm^{-1}, alkyl (C-H stretch) related peak appeared at 2903 cm^{-1} and 2918 cm^{-1}, an amide (N-H stretch) spike was viewed 3362 cm^{-1}, and hydroxyl (O-H stretch) was observed at 3362 cm^{-1} (Singh et al., 2019). The spectrum of MT showed asymmetric and symmetric stretch vibrational bands of primary metformin amines (NH_2) appeared at 3366 cm^{-1} and 3292 cm^{-1}, respectively. Stretch modes of the benzene ring in 2-nitrobenzaldehyde were depicted at 3098-3102 cm^{-1}. The C-H deformation and C=C stretching were observed at 1507 cm^{-1} and 1580 cm^{-1}, respectively. A peak at 1621 cm^{-1} represented metformin-originating primary imines vibrational band (C=N). The notches that arose at 1692 cm^{-1} and 3490 cm^{-1} were associated with carbonyl group (C=O) and secondary amine (N-H), respectively (Al-Qadsy et al., 2020). The peaks pertaining to AT and MT arising appeared in both the spectra obtained by analyzing physical mixture (**Figure 3Ae**) and ES-NPs formulation F5 (**Figure 3Af**); accordingly, they were considered as distinguishing peaks of the drugs. There was no major shift of these distinguishing peaks, and the spectrum of the physical mixture was completely superimposable to that of ES-NPs formulation F5. This suggested that no covalent linkage existed between drug-drug, drug-polymer, or polymer-polymer. Both the drugs remained chemically intact while undergoing the formulation process of electrohydrodynamic jetting and the development of ES-NPs.

DSC thermograms of AT, MT, PVP, HA, Physical mixture, and ES-NPs formulation F5 are shown in **Figure 3B**. A deep and sharp endotherm, corresponding to the melting point of AT, appeared at 170°C in the thermogram of plain AT powder (**Figure 3Ba**). Likewise, a sharp endotherm, appearing at 221°C in the thermogram of plain MT powder, represented its melting point (**Figure 3Bb**). In the thermograms of PVP (**Figure 3Bc**) and HA (**Figure 3Bd**), no sharp endotherm or exotherm was seen depicting their typical amorphous nature. Nevertheless, a downward or endothermic inclination in both the thermograms of PVP and HA in the range of about 70°C-170°C might be ascribed to the escape of physically adsorbed moisture from these samples with increasing temperature. Both the endotherms representing melting points of the drugs also appeared at the same locations in the thermogram of the physical mixture (**Figure 3Be**); thus, they maintained their

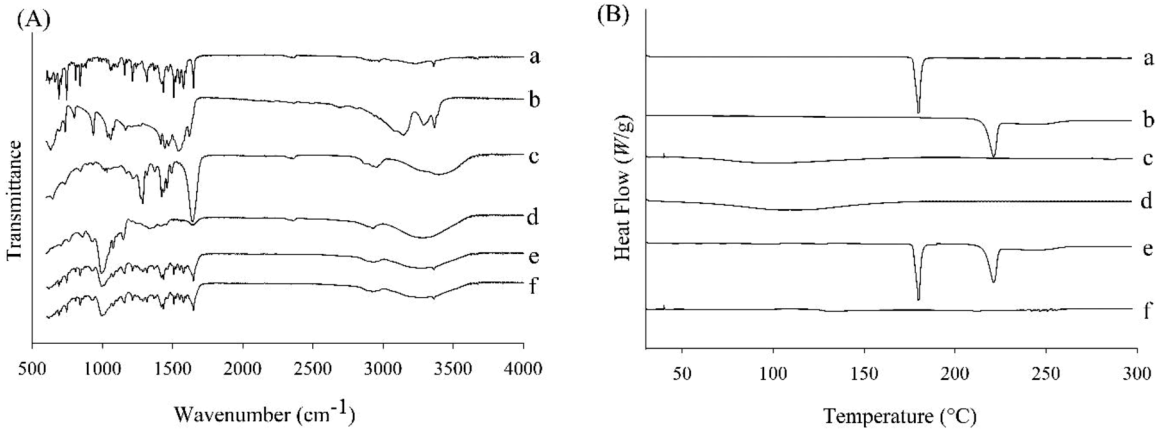

Figure 3. FTIR spectra (A) and DSC thermograms (B) where (a) atorvastatin, (b) metformin, (c) PVP K-30, (d) hyaluronic acid, (e) physical mixture, and (f) ES NPs formulation F5.

crystalline integrity in the physical mixture. On the other hand, both the drugs-related endotherms vanished in the thermogram of ES-NPs formulation F5 (Figure 3Bf). This suggested that both the crystalline drugs were converted into their amorphous counterparts in ES-NPs formulation F5. All the components, the crystalline drugs, and amorphous polymers were dissolved in a solvent system to get a clear solution before electrospraying (Yousaf et al., 2016). The presence of polymeric matrices, PVP, and HA, in the compound solution, exerted a persistent inhibitory influence on the recrystallization of both the drugs during the electrospraying process (Sethia and Squillante, 2004). The drug molecules remained entrapped in the polymeric composite network and could not unite to form nuclei for recrystallization (Mosallaei et al., 2013; Naguib et al., 2014); accordingly, the drugs existed as their amorphous forms in ES-NPs formulation F5. Moreover, it is also well-stated in the previously published literature that the physical state of the drug could be transformed from crystalline to an amorphous state during the electrospraying process (Jahangiri et al., 2017).

All the ES-NPs formulation along with plain drug and marketed products were tested for % release using the USP dissolution apparatus II followed by analysis using RP-HPLC. The amount of drug released as % release is represented in **Figure 4**. For AT, all the formulations showed > 90% release while the marketed product exhibited 80-85%. The plain drug showed less than 55% drug release in all three solvent systems in 60 min. Whereas, for MT, all the ES-NPs formulations showed > 95% release, while the marketed product exhibited 85-90% release and the plain drug showed 80% drug release in all the three solvent systems in 60 min. Another study reported the electrosprayed nano-dispersion for the enhanced dissolution profile and found that the percentage release of ATV was significantly higher (100%) compared to that of the pure drug (70.16 %) during the first 5 min. The comparatively slow release of ATV by ES-NPs reported herein may be due to the incorporation of hyaluronic acid along with PVP acting as a release retarding agent (Jahangiri et al., 2017). The release data was subjected to several mathematical models and based upon the R^2 values the release of AT and MT from the ES-NPs, plain drug, and marketed product, was found to be following the Korsmeyer-Peppas model.

The release behavior of the drugs was in line with their solubility results. All the ES-NPs formulation along with plain drug and marketed

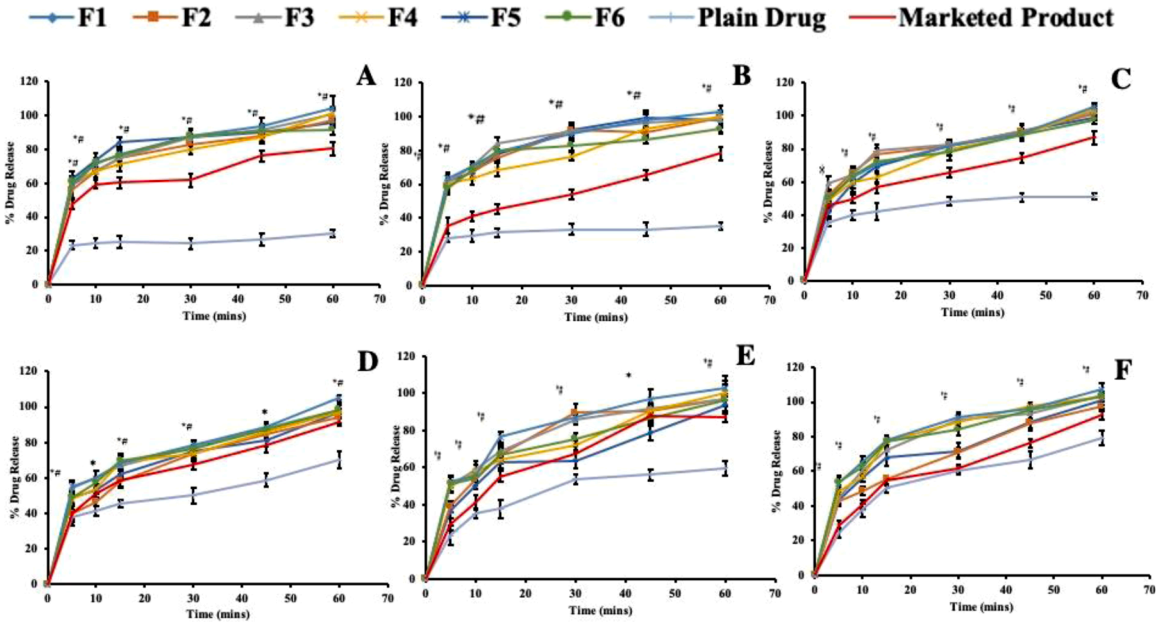

Figure 4. *In vitro* drug release studies of atorvastatin in distilled water (A), phosphate buffer pH 1.2 (B) and phosphate buffer pH 6.8 (C); and metformin in distilled water (D), phosphate buffer pH 1.2 (E) and phosphate buffer pH 6.8 (F). The results are presented as the mean ± S.D. (n = 6). *P<0.05 as compared to the plain drug powder while #P<0.05 as compared to the marketed product.

products were tested for % release using the USP dissolution apparatus II followed by analysis using RP-HPLC. The amount of drug released as % release is represented in Figure 5. For AT, all the formulation showed > 90% release while the marketed product exhibited~ 80-85%. The plain drug showed less than 55% drug release in all the three solvent systems in 60 min. Whereas, for MT, all the ES-NPs formulations showed > 95% release, while the marketed product exhibited 85-90% release and the plain drug showed 80% drug release in all the three solvent systems in 60 min. As compared with plain drug powders, the enhanced release rate of AT or MT from an ES-NPs formulation was owing to decreased particle-size of the formulation that enhanced surface-area of the formulation exposed to the surrounding dissolution medium, and conversion of the crystalline drugs into their amorphous counterparts in the formulation that resulted in the molecular-level diminution of the drug particles (Shilpi et al., 2017). The improvement in solubility and release rate is of utmost significance for adequate absorption and bioavailability of AT. It is expected that via enhancing the solubility and rate of dissolution of the drug, ultimately oral bioavailability would be increased because drug solvency is perceived to be a rate-controlling phase in drug absorption (Löbenberg and Amidon, 2000). Improvement in solubility and release of the poorly soluble drug *via* electrospraying is due to the formation of particles having reduced size, increased surface area, and change of state of the drug from crystalline form to amorphous nature (Hörter and Dressman, 2001). Amorphous forms possess higher solubility and release as compared to crystalline forms (Shayanfar et al., 2013). In particular, ES-NPs formulations F3 and F5 provided the most satisfying results of solubility and release of the drugs; accordingly, they were selected for further *ex vivo* permeation investigations (Talukder et al., 2011).

ANOVA-based methods declared that the release profiles of ES-NPs of both the drugs were significantly improved from pure and commercial drug products (P-value <0.05). Except for MT which showed no significant difference between (pure drug-commercial product) and (F5-commercial product) at 5 mins, 10 mins, and 45 mins (P-value >0.05) in distilled water and phosphate buffer (pH 1.2). In phosphate buffer (pH 6.8) pure drug and commercial products of MT do not display any significant difference at 5 mins till 45 mins of drugs release profile (P-value >0.05). The release data was subjected to several mathematical models and based upon the R^2 values the release of AT and MT from the ES-NPs, plain drug, and marketed product, was found to be following the Korsmeyer-Peppas model. The model-independent approach also confirmed that the release profiles of optimized F5 were not similar or equivalent to the profiles of pure and commercial drug products as f_1 values were >15 and f_2 values were <50. To consider the curves as similar, f_1 values must fall near to 0 whereas, f_2 data is expected to be close to 100. Generally, the f_1 values that are ≤15 and f_2 values which are ≥50 confirm the equivalence of the two respective curves and their performance (Cho et al., 2014). Model-dependent methods suggested that among all the applied kinetic models, Korsmeyer-Peppas has been considered to be the strongest fit model for the release profile, where the coefficient of correlation (R^2) for both the drugs AT-MT is higher in all the three solvent systems as compared to other kinetic models. Diffusion component (n) for AT and MT was found ≤ 0.5 which shows that the drugs obey the Fickian model of diffusion.

The permeability in the best chosen two formulations was determined using Franz diffusion cell and results are shown in **Figure 5**. MT is a BCS class III substance and exhibits poor permeability. Polysorbate 20 (P20), a non-ionic surfactant, exerts a positive effect on permeation of MT; therefore, four formulations F3-0.5%, F3-1%, F5-0.5% and F5-1% were derived from formulation F3 and F5 by the addition of P20 (0.5% and 1%) as shown in Table 1. The shape and size of both the alkyl chains & polar groups of the surfactant is of utmost importance in determining the ability of a surfactant to increase the membrane permeability as reported by Dimitrijevic et al. (2000), where they highlighted the effects of some nonionic surfactants on transepithelial permeability. Polysorbate 85 is a trioleate and due to its bulky structure, it might have some difficulties in penetrating the cell membranes. Generally, polysorbates as a class, have complex structures suggesting that the effects of polysorbates on the permeability of the membrane results from membrane components solubilization instead of penetration. This can be explained by the fact that the polysorbates enhance permeability in a concentration dependent manner and below CMC they only change the physical properties of the membrane. At CMC the surfactant micelles solubilize the membrane lipids while some free surfactant molecules increase the membrane fluidity, thus, enhancing the permeability via transcellular route. Many reports of intestinal absorption enhancing experiments indicated that optimum acyl chain length between C-8 to C-12. For surfactants with C-12 HC chain (like P20), the optimal effects probably corresponded to less bulky structure compared to P-85 and intermediate solubility between oil and water making P20, a potent

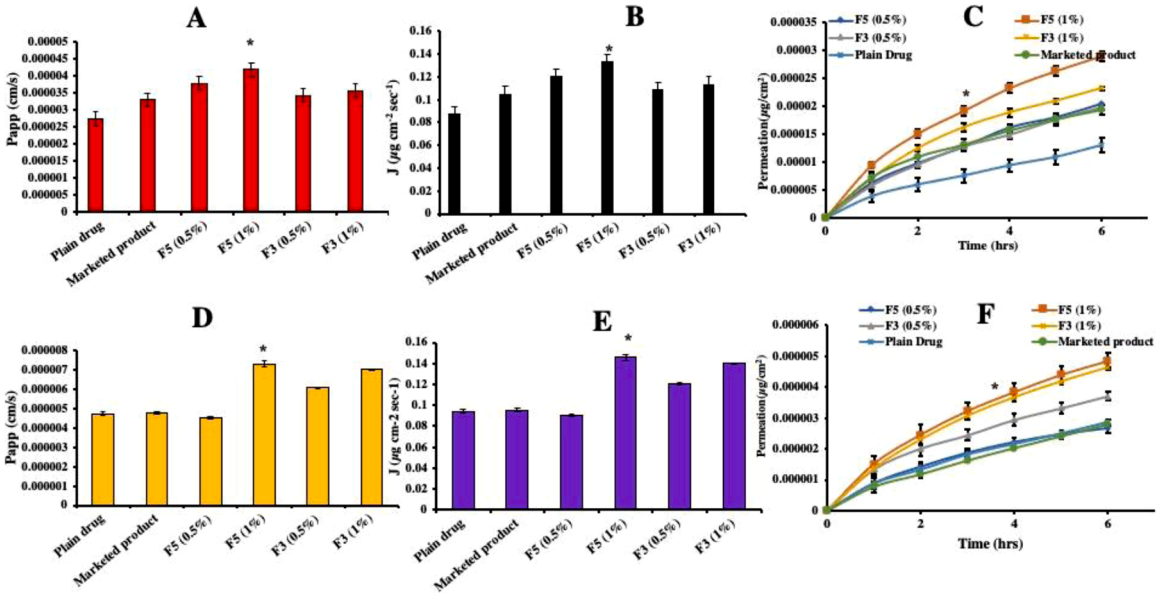

Figure 5. *Ex vivo* permeation studies of final formulations F5 (0.5%, 1%) and F3 (0.5%, 1%) with plain drug and marketed product showing (A) permeability (Papp) of atorvastatin, (B) flux of atorvastatin, (C) cumulative drug permeation of atorvastatin, (D) permeability (Papp) of metformin, (E) flux of metformin, and (F) cumulative drug permeation of metformin. The data is displayed as the mean ± S.D. (n = 3). *P < 0.05 indicate statistically significant difference.

enhancer in the polysorbate series increasing the transcellular permeation across intestinal cells (Dimitrijevic et al., 2000).

For AT, the permeability coefficient (P_{app}) of F5-1% showed the maximum values i.e. 1.53-fold, and 1.27-fold as compared to plain drug and Lipilow, respectively (**Figure 5A**). Similarly, for MT, the maximum P_{app} was found to be 1.60-fold and 1.48-fold respectively for plain drug and Glucophage with F5-1% (**Figure 5D**). Polysorbate 20 (P20), a non-ionic surfactant, exerts a positive effect on permeation of MT; therefore, four formulations F3-0.5%, F3-1%, F5-0.5% and F5-1% were derived from formulation F3 and F5 by the addition of P20 (0.5% and 1%) as shown in Table 1. The results for flux (*J*) (μg cm^{-2} sec^{-1}) for AT, obtained with F5-1%, was 1.52-fold and 1.27-fold higher as compared to plain AT powder and Lipilow respectively (**Figure 5B**). Similarly, for MT, the *J* value obtained with F5-1% was 1.62-fold and 1.49-fold as compared to plain MT powder and respectively (**Figure 5E**). Enhancement ratio (ER) of AT in ES-NPs was also maximum with formulation F5-1% which showed 1.526 and 1.269 in comparison with plain AT powder and Lipilow respectively. Likewise, ER of MT was maximum with same formulation showing 1.607 and 1.474 enhancement in comparison with the MT powder and glucophage respectively.

Permeation of AT and MT with formulations F3 and F5 was evaluated against pure drug powders and marketed products (Lipilow and Glucophage) and the values of enhancement ratio (ER) were recorded. ES-NPs formulation F5-1% resulted in the maximum enhancement of AT as compared to plain AT powder, formulation F3-1%, and marketed product (Lipilow). Likewise, ES-NPs formulation F5-1% showed the maximum permeation of MT as compared to plain MT powder, formulation F3-1%, and marketed product (Glucophage). Moreover, as compared with F5-0.5%, the permeation of the drugs was more with F5-1%. This suggested that higher quantity of P20 (permeation enhancer) in F5-1% resulted in better permeation. Furthermore, as compared with F3-1% (containing PVP/HA, 1/0.66, w/w), threatened permeation with F5-1% (containing PVP/HA, 1/4, w/w) was owing to a higher relative quantity of HA. HA also exerts a positive influence on the permeation of drugs (Sandri et al., 2004). Considering the overall results of solubility, *in vitro* release behavior, and *ex vivo* permeation tests, ES-NPs formulation F5-1% was selected for *in vivo* bioavailability assessment in Sprague-Dawley rats.

Drugs-loaded NPs have been reported to improve the oral bioavailability of poorly water-soluble drugs by increasing solubility and accelerating drug release (Harde et al., 2011). Orally administrated lipophilic and poorly water-soluble drugs using various types of nanoparticles are absorbed and reach the systemic circulation by diffusion through the mucus lining of the gastrointestinal tract, affected by enterocyte surface, epithelial interactions, and cellular infiltrates(Hu et al., 2012). The average plasma concentration-time curves after single oral administration are shown in **Figure 6**. Moreover, the pharmacokinetic parameters are presented in Table 2. Bioavailability assessment was done by considering pharmacokinetic parameters such as $AUC_{(0-\infty)}$, $C_{max,}$ and T_{max}. As compared with AT marketed product (Lipilow), the mean values of $AUC_{(0-\infty)}$, $C_{max,}$ and T_{max} given by ES-NPs formulation F5-1% were significantly high ($p < 0.05$) indicating the 3.5-fold enhancement of bioavailability of AT as compared to Lipilow. Similarly, as compared with MT marketed product (Glucophage), the enhancement of bioavailability of MT with ES-NPs F5-1% was ~2.07-fold. Time to reach maximum plasma concentration (T_{max}), half-life ($t_{1/2}$) and mean residence time (MRT) of AT and MT were also increase with ES-NPs as compared to the marketed products. These results are in accordance with the study reported by where they have found 1.68-fold increase in the oral bioavailability by the use of SLS and HPMC based spray dried solid dispersion (Kwon et al., 2019).

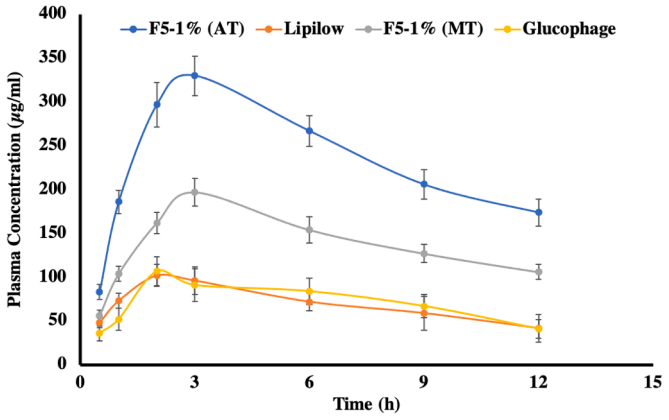

Figure 6. *In vivo* pharmacokinetic studies data in rats showing changes in plasma concentration of AT and MT with time.

The enhanced oral bioavailability of AT was owing to amelioration in solubility and release characteristics of the drug. The improved bioavailability of MT was because of better permeation of the drug by ES-NPs formulation F5-1% due to the presence of HA and P20 (permeation enhancers), conversion of the crystalline MT into its amorphous form (molecular-level size reduction of the drug), and nano-sized formulation particles. Nanoparticles also possess the ability to circumvent elimination by muco-ciliary clearance and to avoid the first-pass metabolism through a lymphatic pathway from the intestinal region infiltrates (Fang et al., 2015). A prolonged MRT of both drugs from ES-NPs is a cumulative effect of delayed T_{max} and increased half-life. This behaviour is expected to be due to the slower but complete drugs release from ES-NPs. Solubility enhancement of APIs along with a modified release from nanoparticulate matrix are supposed to be the key factors involved in the significantly improving the pharmacokinetics profiles of the loaded drugs. Incorporated drugs in the nanoparticles are not exposed to the *in vivo* confrontational factors leading an increased half-life and prolonged mean residence time. Our findings are correlated with the reports presenting that the nanoparticulate delivery of both drugs significantly improves their pharmacokinetics in comparison with other conventional and macro-scaled drug delivery systems. *The in-vivo* behaviour of nanoparticles depends on a number of factors from average particle size to various biological factors such as opsonization. The particle size of nanocarriers cannot be generalized or one cannot suggest any standard size to carry particular drugs to achieve optimal therapeutic effects. Principally, nanomedicines exhibited enhanced pharmacokinetics in comparison with various dosage forms.

4. Conclusion

The electro spraying was successfully employed as a one-step fabrication technique for encapsulating two drugs into a single nano carrier system. The developed nanoparticles were free collected as flowing powder which could either be compressed to tablets or filled in hard gelatin capsule or successful oral administration. The use of FDA approved biocompatible and biodegradable polymers for the development of nanocarriers also helps in minimizing the materials related toxicities. The nanocarriers obtained showed distinct features to enhance the dissolution and oral bioavailability, both *in vitro* and *in vivo* respectively as compared to the marketed products. The significantly ameliorated solubility of AT (a BCS class II drug) and permeability of MT (a BCS class III drug) through these nanocarriers suggests them as a promising platform for the co-delivery of various drug combinations to improve patient compliance. These nanocarriers could be further characterized and developed as dosage form oral administration.

Authors Declaration

The authors declare no conflict of interest.

Credit Statement

Rabia Iqbal: Investigation, analysis and writing the original draft, **Omer Salman Qureshi:** Methodology and validation, **Abid Mehmood Yousaf:** conceptualization, review and editing of original draft, **Syed Atif Raza:** Project administration and validation, **Hafiz Shoaib Sarwar:** Software and formal analysis, **Gul Shahnaz:** Data curation and resources, **Uzma Saleem:** Investigation and analysis and **Muhammad Farhan Sohail:** Conceptualization, supervision, resources, writing editing and review of draft

References

Afzal, I., Sarwar, H.S., Sohail, M.F., Varikuti, S., Jahan, S., Akhtar, S., Yasinzai, M., Satoskar, A.R., Shahnaz, G., 2019. Mannosylated thiolated paromomycin-loaded PLGA nanoparticles for the oral therapy of visceral leishmaniasis. Nanomedicine 14, 387–406.

Al-Qadsy, I., Saeed, W.S., Al-Odayni, A.-B., Ahmed Saleh Al-Faqeeh, L., Alghamdi, A.A., Farooqui, M., 2020. Novel metformin-based schiff bases: synthesis, characterization, and antibacterial evaluation. Materials 13, 514.

Baloch, J., Sohail, M.F., Sarwar, H.S., Kiani, M.H., Khan, G.M., Jahan, S., Rafay, M., Chaudhry, M.T., Yasinzai, M., Shahnaz, G., 2019. Self-nanoemulsifying drug delivery system (SNEDDS) for improved oral bioavailability of chlorpromazine: in vitro and in vivo evaluation. Medicina 55, 210.

Chaudhari, S.P., Dhumal, V., Daswadkar, S., Shirode, D., 2016. Study of formulation variables on bioavailability of metformin gydrochloride. European Journal of Pharmaceutical and Medical research 3, 484–497.

Cho, J.H., Kim, Y.-I., Kim, D.-W., Yousaf, A.M., Kim, J.O., Woo, J.S., Yong, C.S., Choi, H.-G., 2014. Development of novel fast-dissolving tacrolimus solid dispersion-loaded prolonged release tablet. Eur. J. Pharm. Sci. 54, 1–7.

Cyphert, J.M., Trempus, C.S., Garantziotis, S., 2015. Size matters: molecular weight specificity of hyaluronan effects in cell biology. International journal of cell biology 2015.

Dersch, R., Graeser, M., Greiner, A., Wendorff, J.H., 2007. Electrospinning of nanofibres: towards new techniques, functions, and applications. Australian journal of chemistry 60, 719–728.

Dimitrijevic, D., Shaw, A.J., Florence, A.T., 2000. Effects of some non-ionic surfactants on transepithelial permeability in Caco-2 cells. Journal of pharmacy and pharmacology 52, 157–162.

Din, F.u., Choi, J.Y., Kim, D.W., Mustapha, O., Kim, D.S., Thapa, R.K., Ku, S.K., Youn, Y. S., Oh, K.T., Yong, C.S., 2017. Irinotecan-encapsulated double-reverse thermosensitive nanocarrier system for rectal administration. Drug Deliv 24, 502–510.

Fang, G., Tang, B., Chao, Y., Zhang, Y., Xu, H., Tang, X., 2015. Improved oral bioavailability of docetaxel by nanostructured lipid carriers: in vitro characteristics, in vivo evaluation and intestinal transport studies. RSC advances 5, 96437–96447.

Franco, P., De Marco, I., 2020. The Use of Poly (N-vinyl pyrrolidone) in the Delivery of Drugs: A Review. Polymers 12, 1114.

Ghafar, H., Khan, M.I., Sarwar, H.S., Yaqoob, S., Hussain, S.Z., Tariq, I., Madni, A.U., Shahnaz, G., Sohail, M.F., 2020. Development and characterization of bioadhesive film embedded with lignocaine and calcium fluoride nanoparticles. AAPS PharmSciTech 21, 1–12.

Grundy, S.M., Brewer Jr., H.B., Cleeman, J.I., Smith Jr., S.C., Lenfant, C., 2004. Definition of metabolic syndrome: report of the National Heart, Lung, and Blood Institute/American Heart Association conference on scientific issues related to definition. Circulation 109, 433–438.

Hameed, M., Rasul, A., Nazir, A., Yousaf, A.M., Hussain, T., Khan, I.U., Abbas, G., Abid, S., Yousafi, Q.u.A., Ghori, M.U., 2020. Moxifloxacin-loaded electrospun polymeric composite nanofibers-based wound dressing for enhanced antibacterial activity and healing efficacy. International Journal of Polymeric Materials and Polymeric Biomaterials 1–9.

Hörter, D., Dressman, J., 2001. Influence of physicochemical properties on dissolution of drugs in the gastrointestinal tract. Advanced drug delivery reviews 46, 75–87.

Hu, K., Cao, S., Hu, F., Feng, J., 2012. Enhanced oral bioavailability of docetaxel by lecithin nanoparticles: preparation, in vitro, and in vivo evaluation. International Journal of Nanomedicine 7, 3537–3545.

Hu, L., Tang, X., Cui, F., 2004. Solid lipid nanoparticles (SLNs) to improve oral bioavailability of poorly soluble drugs. J. Pharm. Pharmacol. 56, 1527–1535.

Ibrahim, H.M., Klingner, A., 2020. A review on electrospun polymeric nanofibers: Production parameters and potential applications. Polymer Testing 90, 106647–106665.

Islam, A., Ain, Q., Munawar, A., Corrêa Junior, J.D., Khan, A., Ahmad, F., Demicheli, C., Shams, D.F., Ullah, I., Sohail, M.F., 2020. Reactive oxygen species generating photosynthesized ferromagnetic iron oxide nanorods as promising antileishmanial agent. Nanomedicine 15, 755–771.

Jahangiri, A., Adibkia, K., 2016. Applications of electrospinning/electrospraying in drug delivery. Bioimpact 6, 1–2.

Jahangiri, A., Barzegar-Jalali, M., Javadzadeh, Y., Hamishehkar, H., Adibkia, K., 2017. Physicochemical characterization of atorvastatin calcium/ezetimibe amorphous nano-solid dispersions prepared by electrospraying method. Artificial cells, nanomedicine, and biotechnology 45 1138–1145.

Jaworek, A., 2007. Micro-and nanoparticle production by electrospraying. Powder technology 176, 18–35.

Jaworek, A., Sobczyk, A.T., 2008. Electrospraying route to nanotechnology: An overview. Journal of electrostatics 66, 197–219.

JS, P., Kadam, D., Marapur, S., Kamalapur, M., 2010. Inclusion complex system; a novel technique to improve the solubility and bioavailability of poorly soluble drugs: a review. International Journal of Pharmaceutical Sciences Review and Research 2, 29–34.

Kumar, R., Gokulakrishnan, N., Kumar, R., Krishna, V.M., Saravanan, A., Supriya, S., Somanathan, T., 2015. Can Be a Bimetal Oxide ZnO—MgO Nanoparticles Anticancer Drug Carrier and Deliver? Doxorubicin Adsorption/Release Study. Journal of nanoscience and nanotechnology 15, 1543–1553.

Kwon, J., Giri, B.R., Song, E.S., Bae, J., Lee, J., Kim, D.W., 2019. Spray-dried amorphous solid dispersions of atorvastatin calcium for improved supersaturation and oral bioavailability. Pharmaceutics 11, 461.

Leuner, C., Dressman, J., 2000. Improving drug solubility for oral delivery using solid dispersions. European journal of Pharmaceutics and Biopharmaceutics 50, 47–60.

Löbenberg, R., Amidon, G.L., 2000. Modern bioavailability, bioequivalence and biopharmaceutics classification system. New scientific approaches to international regulatory standards. Eur. J. Pharm. Biopharm. 50, 3–12.

Malinowski, J.M.J.A.j.o.h.-s.p., 1998. Atorvastatin: a hydroxymethylglutaryl-coenzyme A reductase inhibitor. 55, 2253-2267.

Mortensen, M.B., Kulenovic, I., Falk, E., 2016. Statin use and cardiovascular risk factors in diabetic patients developing a first myocardial infarction. Cardiovascular Diabetology 15, 1–8.

Mosallaei, N., Jaafari, M.R., Hanafi-Bojd, M.Y., Golmohammadzadeh, S., Malaekeh-Nikouei, B., 2013. Docetaxel-loaded solid lipid nanoparticles: preparation, characterization, in vitro, and in vivo evaluations. J. Pharm. Sci. 102, 1994–2004.

Mustapha, O., Din, F.U., Kim, D.W., Park, J.H., Woo, K.B., Lim, S.-J., Youn, Y.S., Cho, K. H., Rashid, R., Yousaf, A.M., 2016. Novel piroxicam-loaded nanospheres generated by the electrospraying technique: physicochemical characterisation and oral bioavailability evaluation. Journal of microencapsulation 33, 323–330.

Naguib, Y.W., Rodriguez, B.L., Li, X., Hursting, S.D., Williams III, R.O., Cui, Z., 2014. Solid lipid nanoparticle formulations of docetaxel prepared with high melting point triglycerides: in vitro and in vivo evaluation. Mol. Pharm. 11, 1239–1249.

Nikolakakis, I., Partheniadis, I., 2017. Self-emulsifying granules and pellets: composition and formation mechanisms for instant or controlled release. Pharmaceutics 9, 1–27.

Nozawa, Y., Mizumoto, T., Higashide, F., 1984. Increasing dissolution rate of phenacetin by roll mixing with polyvinyl pyrrolidone. Yakuzaigaku 44, 134–140.

Nyström, C., Westerberg, M., 1986. The use of ordered mixtures for improving the dissolution rate of low solubility compounds&. J. Pharm. Pharmacol. 38, 161–165.

Reddy, M.S., Reddy, N.S., Reddy, S.M., 2014. Solubility enhancement of poorly water soluble drug efavirenz by solid self emulsifying drug delivery systems. IJPRR 3, 20–28.

Sandri, G., Rossi, S., Ferrari, F., Bonferoni, M.C., Zerrouk, N., Caramella, C., 2004. Mucoadhesive and penetration enhancement properties of three grades of hyaluronic acid using porcine buccal and vaginal tissue, Caco-2 cell lines, and rat jejunum. Journal of pharmacy and pharmacology 56, 1083–1090.

Sapkal, S., Narkhede, M., Babhulkar, M., Mehetre, G., Rathi, A., 2013. Natural polymers: Best carriers for improving bioavailability of poorly water soluble drugs in solid dispersions. Marmara Pharmaceutical Journal 17, 65–72.

Sareen, S., Mathew, G., Joseph, L., 2012. Improvement in solubility of poor water-soluble drugs by solid dispersion. International journal of pharmaceutical investigation 2, 12–17.

Sarwar, H.S., Varikuti, S., Sohail, M.F., Sarwar, M., Akhtar, S., Satoskar, A.R., Shahnaz, G., 2020. Oral delivery and enhanced efficacy of antimonal drug through macrophage-guided multifunctional nanocargoes against visceral Leishmaniasis. European Journal of Pharmaceutics and Biopharmaceutics 152, 307–317.

Sattar, N., Preiss, D., Murray, H.M., Welsh, P., Buckley, B.M., de Craen, A.J., Seshasai, S. R.K., McMurray, J.J., Freeman, D.J., Jukema, J.W., 2010. Statins and risk of incident diabetes: a collaborative meta-analysis of randomised statin trials. The Lancet 375, 735–742.

Sethia, S., Squillante, E., 2004. Solid dispersion of carbamazepine in PVP K30 by conventional solvent evaporation and supercritical methods. Int. J. Pharm. 272, 1–10.

Shayanfar, A., Ghavimi, H., Hamishekar, H., Jouyban, A., 2013. Coamorphous atorvastatin calcium to improve its physicochemical and pharmacokinetic properties. J. Pharm. Pharm. Sci. 16, 577–587.

Shilpi, D., Kushwah, V., Agrawal, A.K., Jain, S., 2017. Improved stability and enhanced oral bioavailability of atorvastatin loaded stearic acid modified gelatin nanoparticles. Pharm. Res. 34, 1505–1516.

Singh, S.Y., Shirodkar, R.K., Verma, R., Kumar, L., 2019. Enhancement in dissolution rate of atorvastatin trihydrate calcium by formulating its porous tablet using sublimation technique. Journal of Pharmaceutical Innovation 15, 498–520.

Snetkov, P., Morozkina, S., Uspenskaya, M., Olekhnovich, R., 2019. Hyaluronan-Based Nanofibers: Fabrication, Characterization and Application. Polymers 11, 2036–2061.

Sohail, M.F., Javed, I., Hussain, S.Z., Sarwar, S., Akhtar, S., Nadhman, A., Batool, S., Bukhari, N.I., Saleem, R.S.Z., Hussain, I., 2016. Folate grafted thiolated chitosan enveloped nanoliposomes with enhanced oral bioavailability and anticancer activity of docetaxel. Journal of Materials Chemistry B 4, 6240–6248.

Solanki, S.S., Sarkar, B., Dhanwani, R.K., 2012. Microemulsion drug delivery system: for bioavailability enhancement of ampelopsin. ISRN pharmaceutics 2012.

Sridhar, R., Ramakrishna, S., 2013. Electrosprayed nanoparticles for drug delivery and pharmaceutical applications. Biomatter 3, e24281–e24293.

Stepensky, D., Friedman, M., Srour, W., Raz, I., Hoffman, A., 2001. Preclinical evaluation of pharmacokinetic–pharmacodynamic rationale for oral CR metformin formulation. J. Control. Release 71, 107–115.

Sun, R., Shen, C., Shafique, S., Mustapha, O., Hussain, T., Khan, I.U., Mehmood, Y., Anwer, K., Shahzad, Y., Yousaf, A.M., 2020a. Electrosprayed Polymeric Nanospheres for Enhanced Solubility, Dissolution Rate, Oral Bioavailability and Antihyperlipidemic Activity of Bezafibrate. International Journal of Nanomedicine 15, 705.

Sun, R., Shen, C., Shafique, S., Mustapha, O., Hussain, T., Khan, I.U., Mehmood, Y., Anwer, K., Shahzad, Y., Yousaf, A.M., 2020b. Electrosprayed Polymeric Nanospheres for Enhanced Solubility, Dissolution Rate, Oral Bioavailability and Antihyperlipidemic Activity of Bezafibrate. International Journal of Nanomedicine 15, 705–715.

Talukder, R., Reed, C., Dürig, T., Hussain, M., 2011. Dissolution and solid-state characterization of poorly water-soluble drugs in the presence of a hydrophilic carrier. AAPS PharmSciTech 12, 1227–1233.

Tang, K., Gomez, A., 1994. Generation by electrospray of monodisperse water droplets for targeted drug delivery by inhalation. Journal of aerosol science 25, 1237–1249.

Wang, Y., Snee, R.D., Keyvan, G., Muzzio, F.J.J.D.d., pharmacy, i., 2016. Statistical comparison of dissolution profiles. 42, 796-807.

Wu, L., Parhofer, K.G., 2014. Diabetic dyslipidemia. Metabolism 63, 1469–1479.

Yousaf, A.M., Kim, D.W., Oh, Y.-K., Yong, C.S., Kim, J.O., Choi, H.-G., 2015. Enhanced oral bioavailability of fenofibrate using polymeric nanoparticulated systems: physicochemical characterization and in vivo investigation. International journal of nanomedicine 10, 1819.

Yousaf, A.M., Mustapha, O., Kim, D.W., Kim, D.S., Kim, K.S., Jin, S.G., Yong, C.S., Youn, Y.S., Oh, Y.-K., Kim, J.O., 2016. Novel electrosprayed nanospherules for enhanced aqueous solubility and oral bioavailability of poorly water-soluble fenofibrate. International journal of nanomedicine 11, 213–221.

Yousaf, A.M., Ramzan, M., Shahzad, Y., Mahmood, T., Jamshaid, M., 2019. Fabrication and in vitro characterization of fenofibric acid-loaded hyaluronic acid–polyethylene glycol polymeric composites with enhanced drug solubility and dissolution rate. International Journal of Polymeric Materials and Polymeric Biomaterials 68, 510–515.

Zeb, A., Qureshi, O.S., Kim, H.S., Kim, M.S., Kang, J.H., Park, J.S., Kim, J.K., 2017. High payload itraconazole-incorporated lipid nanoparticles with modulated release property for oral and parenteral administration. Journal of Pharmacy and Pharmacology 69, 955–966.

Zhang, Y., Huo, M., Zhou, J., Zou, A., Li, W., Yao, C., Xie, S., 2010. DDSolver: an add-in program for modeling and comparison of drug dissolution profiles. The AAPS journal 12, 263–271.

Zu, Y., Li, N., Zhao, X., Li, Y., Ge, Y., Wang, W., Wang, K., Liu, Y., 2014. In vitro dissolution enhancement of micronized L-nimodipine by antisolvent re-crystallization from its crystal form H. Int. J. Pharm. 464, 1–9.